

## ON THE APPLICATION OF BIOT'S THEORY TO ACOUSTIC WAVE PROPAGATION IN SNOW

J.B. Johnson

Geophysical Institute, University of Alaska, Fairbanks, AK (U.S.A.)

(Received November 16, 1981; accepted in revised form February 8, 1982)

### ABSTRACT

*A fluid-saturated, elastic, porous media model is used to describe acoustic wave propagation in snow. This model predicts the existence of two dilatational waves and a shear wave. In homogeneous, isotropic snow the two dilatational waves are uncoupled from one another but involve coupled motion between the interstitial air and ice skeleton. Dilatational waves of the first kind and shear waves are slightly dispersive and attenuated with distance. Dilatational waves of the second kind are strongly dispersive and highly attenuated. The model also predicts that the wave impedance for snow is close to that of air and that snow strongly absorbs acoustic wave energy.*

*Available experimental phase velocity, impedance and attenuation data support the calculated results. Phase velocity measurements indicate three identifiable categories: fast dilatational waves (phase velocity  $\geq 500$  m/s), slow dilatational waves (phase velocity  $< 500$  m/s) and shear waves. Wave impedance and attenuation measurements illustrate the low impedance, highly absorbing characteristics of snow. Additional impedance, attenuation and phase velocity data are required to further test and improve the model.*

### INTRODUCTION

Developing an understanding of the propagation

of acoustic waves in snow has been the object of theoretical and experimental work by various investigators. This interest is the result of a desire to use acoustic techniques for: nondestructive methods of snow texture classification; the determination of mechanical parameters for snow; developing effective methods of explosive control for snow slopes; and monitoring acoustical emissions.

Development of textural classification techniques and determination of the appropriate mechanical parameters for snow require an accurate acoustic propagation model. Earlier acoustic wave propagation models have used either porous media representations which assumed a rigid ice skeleton, or used continuum elastic or inelastic models (Nakaya, 1959a, 1959b, 1961; Ishida, 1965; Smith, 1965; Yen and Fan, 1966; Chae, 1966; Smith, 1969). These models do not adequately explain observed wave propagation phenomena in snow. Air pressure waves, propagating in the interstitial pore space, and dilatational and shear stress waves, propagating in the ice skeleton, have been detected in snow (Oura, 1952; Smith, 1965; Yamada et al., 1974; Gubler, 1977). However, neither the porous media or continuum models can explain all three wave propagation modes. In this paper, a model is presented which is more representative of acoustical wave propagation in snow. It utilizes the work of Biot (1956a, 1956b) to treat the snow as a porous material with an elastic skeleton saturated by a compressible viscous fluid (air).

In the following sections, the equations of motion

for acoustic wave propagation in porous media, and their solutions, are presented and adapted to snow. The characteristics of the solutions describing acoustic waves in snow are discussed in detail and compared with the experimental results of Ōura (1952a), Smith (1965), Yamada et al. (1974), Bogorodskii et al. (1974) and Johnson (1978).

## ACOUSTIC WAVES IN SNOW

### Equations of motion

Biot (1956a and b) developed stress–strain relations for a porous aggregate including the effects of fluid pressure and dilatation. He considered the dynamics of the material and the coupling between fluid and solid under the assumptions that the material is statistically homogeneous and isotropic in the region of interest, behaves in a linearly elastic manner and that thermoelastic effects are negligible. The macroscopic stress–strain relation for the medium was derived by assuming the strain energy function, and the coupling effect between the elastic skeleton and compressible fluid was accounted for by introducing a mass coupling parameter into the kinetic energy of the system. Dissipation of energy by the viscous fluid was expressed in terms of the relative velocity between the fluid and solid; internal friction of the solid material was neglected.

The upper bound of frequency for which Biot's model applies is that at which the wavelengths are the order of magnitude of (or greater than) the linear cross-sectional dimensions of the pores (Biot, 1956b). This frequency limitation is imposed because the effects of scattering become important as the wavelength approaches the pore size.

The constitutive relations describing the porous material are:

$$\begin{aligned} \sigma_{ij} &= (Ae + Qe)\delta_{ij} + 2Ne_{ij}, \\ s &= Qe + Re, \end{aligned} \quad (1)$$

where  $\sigma_{ij}$  is the stress in the solid framework,  $s$  is the fluid pore pressure,  $e$  and  $\epsilon$  are the dilatations of the solid and fluid,  $e_{ij}$  is the strain in the solid, and  $\delta_{ij}$  is the Kroneker delta.  $A$  is an elastic constant and  $N$  is the shear modulus for the solid. The coefficient  $R$

is a measure of the pressure on the fluid required to force a certain volume of the fluid into the aggregate while the total volume remains constant. The coefficient  $Q$  is of the nature of a coupling between the volume change of the fluid and that of the solid (Biot, 1956a). These parameters are inherently positive and satisfy the inequality

$$(A + 2N)R - Q^2 > 0.$$

Biot derived the equations of motion for the porous media, using Lagrangian equations, which have the form

$$\begin{aligned} N\nabla^2 \mathbf{u} + \nabla((A+N)\nabla \cdot \mathbf{u} + Q\nabla \cdot \mathbf{U}) &= \partial^2/\partial t^2(\rho_{11}\mathbf{u} \\ &+ \rho_{12}\mathbf{U}) + b(\theta) \partial/\partial t(\mathbf{u} - \mathbf{U}), \\ \nabla(Q\nabla \cdot \mathbf{u} + R\nabla \cdot \mathbf{U}) &= \partial^2/\partial t^2(\rho_{12}\mathbf{u} + \rho_{22}\mathbf{U}) \\ &- b(\theta) \partial/\partial t(\mathbf{u} - \mathbf{U}), \end{aligned} \quad (2)$$

where  $\mathbf{u}$  is the displacement vector for the solid skeleton and  $\mathbf{U}$  is the displacement vector for the fluid. The parameters  $\rho_{11}$ ,  $\rho_{22}$  and  $\rho_{12}$  are dynamic coefficients that take into account the inertial effect of the moving fluid. These parameters are related to the mass densities of the solid ( $\rho_s$ ) and the fluid ( $\rho_f$ ) by the equations

$$\rho = \rho_{11} + 2\rho_{12} + \rho_{22} = (1 - \beta)\rho_s + \beta\rho_f,$$

where  $\rho$  is the density of the aggregate,  $\rho_s$  is the density of the solid material,  $\rho_f$  is the density of the fluid material, and where

$$\rho_{11} + \rho_{12} = (1 - \beta)\rho_s,$$

$$\rho_{12} + \rho_{22} = \beta\rho_f.$$

The parameters satisfy the inequalities

$$\begin{aligned} \rho_{11} &> 0, & \rho_{22} &\geq 0, \\ \rho_{12} &\leq 0, & \rho_{11}\rho_{22} - \rho_{12}^2 &> 0, \end{aligned}$$

and

$$(A + 2N)\rho_{11} + R\rho_{22} - 2Q\rho_{12} > 0,$$

where  $\beta$  is the effective porosity of the medium and  $\rho_{12}$  is an apparent mass term that acts as a coupling term between fluid and solid and whose influence on the dynamic relations increases as the fluid flow becomes more restricted in the material. The dissipation of an acoustic wave caused by fluid

friction is taken into account through the parameter  $b(\theta)$  which is related to the permeability ( $B$ ), the effective porosity ( $\beta$ ) and the fluid viscosity  $\nu(\theta)$  by the equation

$$b(\theta) = \beta^2 \nu(\theta) / B. \quad (3)$$

The frequency dependent correction term,  $\nu(\theta)$ , serves as a measure of the deviation from Poiseuille-flow friction as a function of the nondimensional frequency parameter,  $\theta = d (\omega/\nu)^{1/2}$ ;  $\omega$  is the frequency of the disturbance,  $\nu$  is the kinematic viscosity of the fluid and  $d$  is a characteristic linear dimension of the pore cross-section. Pore geometry is described by a structure factor ( $T$ ) which is usually determined experimentally from dispersion and attenuation data (Biot, 1956b). The physical significance of these parameters has been discussed by Biot (1941, 1956a, 1956b), Biot and Willis (1957) and Yew and Jogi (1976) and will not be repeated here.

### Solutions to the equations of motion

Biot's theory predicts the existence of two attenuated dilatational waves and an attenuated shear wave. The characteristics of these waves in snow can be determined by applying Deresiewicz and Rice's (1962) solutions of Biot's equations, in which Helmholtz's method is used to describe the displacement vectors for the solid and fluid components of the aggregate,

$$\begin{aligned} \mathbf{u} &= \text{grad}(\phi_1 + \phi_2) + \text{curl} \mathbf{H}, \\ \mathbf{U} &= \text{grad}(\mu_1 \phi_2 + \mu_2 \phi_2) + \text{curl}(\alpha \mathbf{H}). \end{aligned} \quad (4)$$

The scalar potentials  $\phi_1$  and  $\phi_2$  describe the propagation characteristics of dilatational waves of the first and second kind, respectively.  $\mathbf{H}$  describes the propagation characteristics of shear waves. The functions  $\mu_1$ ,  $\mu_2$  and  $\alpha$  depend on the mechanical parameters describing the porous medium and frequency. For plane wave propagation the scalar potentials and  $\mathbf{H}$  are given by

$$\begin{aligned} \phi_1 &= D \exp[i(\omega t - \delta_1 x_j)] \\ \phi_2 &= E \exp[i(\omega t - \delta_2 x_j)] \\ \mathbf{H} &= \mathbf{F} \exp[i(\omega t - \delta_3 x_j)], \quad j = 1, 2, 3, \end{aligned} \quad (5)$$

where  $D$ ,  $E$  and  $\mathbf{F}$  are constants. The solutions and relationships between the wave parameters ( $\delta_K$ ,  $\mu_1$ ,

$\mu_2$ ,  $\alpha$ ) and material parameters ( $A$ ,  $N$ ,  $R$ ,  $Q$ ,  $b(\theta)$ ) are described in detail by Deresiewicz and Rice (1962). These solutions to Biot's equations indicate that dilatational waves of the first and second kind and shear waves affect the displacements in both the fluid and the solid (eqns. (4)). This means that wave propagation motions in the fluid and solid are coupled to each other. Equations (5) show that the three wave types propagate independently from one another with different propagation constants ( $\delta_1$ ,  $\delta_2$  and  $\delta_3$ ) and the same angular frequency ( $\omega$ ).

### Determining the mechanical parameters for snow

The dynamic nature of a porous material is determined by the parameters  $A$ ,  $N$ ,  $R$ , and  $Q$ . These parameters are calculated from four measurable coefficients ( $N$ ,  $\kappa$ ,  $\tau$ ,  $\gamma$ ) through the relations

$$\begin{aligned} N &= v_s^2 \rho_d, \\ A &= (\gamma/\kappa + \beta^2 + (1 - 2\beta)(1 - \tau/\kappa))/(\gamma + \tau - \tau^2/\kappa) \\ &\quad - 2N/3, \\ Q &= (\beta(1 - \beta - \tau/\kappa))/(\gamma + \tau - \tau^2/\kappa), \\ R &= \beta^2/(\gamma + \tau - \tau^2/\kappa), \end{aligned} \quad (6)$$

where  $N$  is the shear modulus of the bulk material,  $v_s$  is the propagation velocity for shear waves in the porous aggregate,  $\rho_d$  is the density of the drained aggregate,  $\kappa$  is the jacketed compressibility of the porous aggregate (the pore pressure of the aggregate sample is held constant, 0 Pa, during the application of an external pressure),  $\tau$  is the unjacketed compressibility (the sample's pore pressure equals the applied pressure), and  $\gamma$  is a measure of the fluid per unit pressure that enters the pores under the application of fluid pressure (Biot and Willis, 1957).

The physical interpretation and methods for determining  $\gamma$ ,  $\kappa$ ,  $\tau$ ,  $\mu$  and  $\beta$  from static tests have been discussed by Biot and Willis (1957) and Yew and Jogi (1978). However, static tests are not suitable when the material properties of the porous media are dependent on loading rate as is the case for snow (Mellor, 1964, 1974). Johnson (1978) has shown that the Biot-Willis coefficients can be determined for snow using dynamic tests and the relations

$$\begin{aligned} N &= v_s^2 \rho_d, \quad 1/\kappa = (Y_s N)/(9N - 3Y_s), \\ \tau &\approx C_i, \quad \gamma = \beta(C_{\text{air}} - \tau), \end{aligned} \quad (7)$$

TABLE 1

Calculated Biot-Willis coefficients for snow assuming a fluid-saturated porous material model. Young's Modulus and the shear modulus data were taken from Smith (1965) and Yamada et al. (1974)

$\rho$ Density (kg/m <sup>3</sup> )	$Y_s$ Young's modulus (GPa)	$\beta$ Porosity	$1/\kappa$ (MPa)	$\tau$ (Pa)	$\gamma$ (MPa <sup>-1</sup> )	$A$ (MPa)	$N$ (MPa)	$Q$ (KPa)	$R$ (KPa)
<i>Equitemperature metamorphosed snow</i>									
210	0.03	0.772	37	0.837	7.61	29.3	11	22.8	78.2
250	0.085	0.728	50	0.837	7.19	26.3	35	27.1	73.7
300	0.2	0.674	200	0.837	6.65	150	75	31.2	68.3
350	0.423	0.620	241	0.837	6.12	125	175	36.5	62.8
410	0.427	0.554	275	0.837	5.47	160	172	42.8	56.1
440	0.61	0.522	416	0.837	5.15	247	253	44.9	52.9
508	1.33	0.448	571	0.837	4.42	173	598	51.1	45.4
551	2.22	0.401	1532	0.837	3.96	944	882	47.7	40.6
600	2.73	0.348	2275	0.837	3.43	1575	1050	46.8	35.3
<i>Temperature gradient metamorphosed snow</i>									
360	0.28	0.608	97.6	0.837	6.0	6	137	39.0	61.6
400	0.396	0.565	153	0.837	5.58	30	185	43.0	57.2
500	0.865	0.456	431	0.837	4.5	184	371	51.5	46.2

where  $Y_s$  is the dynamic Young's modulus and  $C_i$  and  $C_{air}$  are the bulk compressibility for ice and air. Because  $\tau \ll \gamma \ll 1/\kappa$  the errors in determining  $\tau$  or  $\gamma$  must be large before they significantly affect the calculated values of  $A$ ,  $N$ ,  $R$  and  $Q$  (eqns. (6)). Equations (7), the dynamic measurements of  $N$  and  $Y_s$  by Smith (1965), and the wave propagation velocity measurements by Yamada et al. (1974) can be used to calculate representative values of  $A$ ,  $N$ ,  $R$  and  $Q$  for snow (Table 1). The effective porosity ( $\beta$ ) values in Table 1 were calculated from the relationship

$$\beta = 1 - (\rho_{sn}/\rho_i)$$

where  $\rho_i$  and  $\rho_{sn}$  are the densities of ice and snow. The relative importance of the constituent elements of snow (the ice framework and air-filled pore space) is illustrated by the changes in the material parameters with respect to density (porosity). An increase in snow density is associated with an increase in the dilatational and shear parameters  $A$  and  $N$ , an initial increase in  $Q$  (until  $\rho = 508 \text{ kg/m}^3$ ) then a decrease, and a decrease in  $R$  (Table 1). These results demonstrate that the contribution of the fluid (air) to the mechanical behavior of snow becomes more significant as the porosity increases. It is also apparent that

the ice framework dominates the mechanical behavior of snow at high densities (low porosity).

### THEORETICAL PREDICTION OF THE ACOUSTIC RESPONSE OF SNOW

The acoustic wave propagation properties of snow are described by the phase velocities and attenuation characteristics of the three wave types and the wave impedance of snow. The phase velocities for the two dilatational waves and shear wave are given by the ratio of the angular frequency to the real part of the propagation constant:

$$C_k = \omega/\text{Re}(\delta_k), \quad k = 1, 2, 3.$$

Attenuation coefficients for the wave types are given by the imaginary part of the propagation constant;

$$\alpha_k = \text{Im}(\delta_k), \quad k = 1, 2, 3.$$

The wave impedance ( $W$ ) is a ratio between the pressure and normal particle velocity at a point on the surface of a sample. It is a material constant and is independent of position in a homogeneous, isotropic sample. If the pressure and particle velocity are not in phase then  $W$  is a complex quantity where

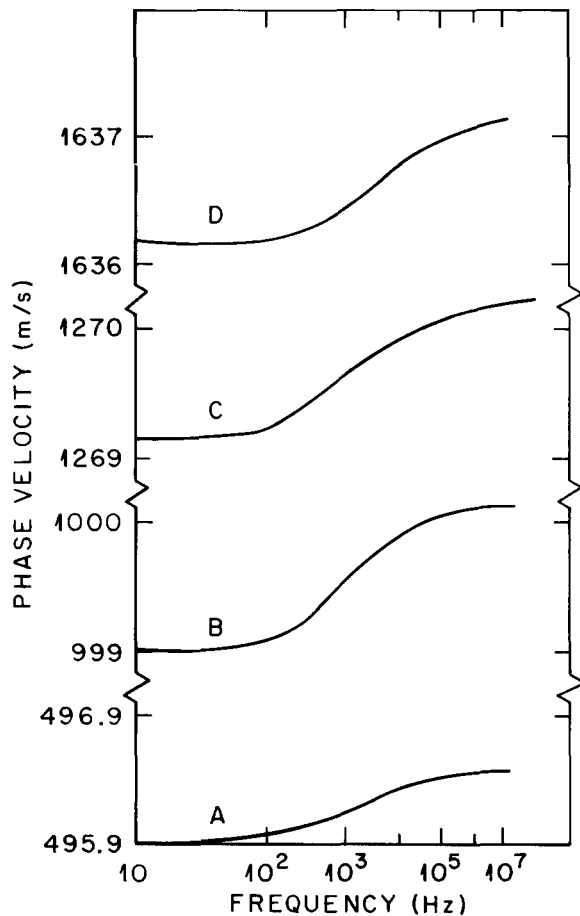
$$W = W_r + i W_i.$$

$W_r$  is the resistance and is a positive value when acoustic energy is transmitted into the snow.  $W_i$  is the reactance and depends on the phase difference between the pressure and partial velocity. The ratio of the acoustic wave resistance of the reflecting medium (snow) to that of the medium that carries the incident wave (air) is given by

$$W/\rho_0 c_0 = W_r/\rho_0 c_0 + i W_i/\rho_0 c_0.$$

The characteristic impedance of air is  $\rho_0 c_0$  where  $\rho_0$  is the air density and  $c_0$  is the acoustic wave propagation velocity in air. In this article calculated and measured impedance data are presented as the ratio of the wave impedance of snow to the characteristic impedance of air.

In this study representative values of permeability ( $B$ ), structure factor ( $\Upsilon$ ) and the material parameters



$A, N, Q, R$  for snow from Ishida (1965) and Johnson (1978) were used to calculate the theoretical dispersion, attenuation, and wave impedance curves. The calculated curves for the phase velocity dispersion and attenuation of dilatational waves of the first and second kind and shear waves, where  $\rho_{12} = 0$ , are shown in Figs. 1--10. Dilatational waves of the first kind and shear waves show very little dispersion and their phase velocities increase with increasing frequency and snow density (Figs. 1 and 3). Both wave types are slightly attenuated. Amplitude attenuation is dependent not only on the frequency but also on path length, density and air permeability (Figs. 4--6, 8 and 9). Attenuation coefficients increase with increasing frequency. They also increase, for a given frequency, with decreasing snow density and air permeability in the low frequency range (Figs. 5, 6, 8 and 9). At high frequencies, permeability decreases result in larger attenuation coefficients at a given frequency (Figs. 8 and 9). Dilatational waves of the second kind are strongly dispersive and attenuated. Their phase velocities increase with frequency but

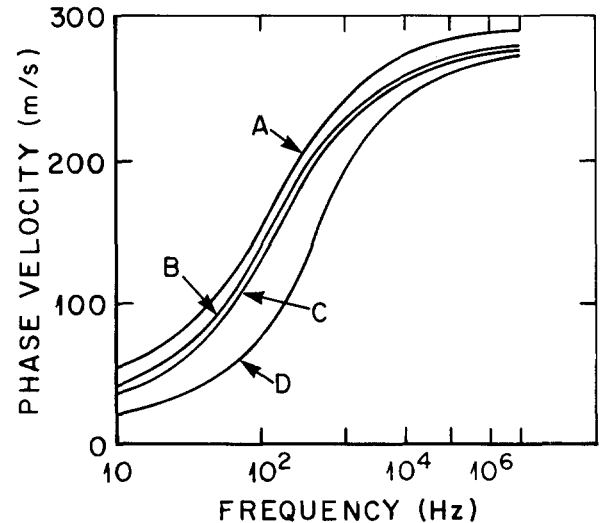


Fig. 2. Predicted phase velocity dispersion for dilatational waves of the second kind. The density, permeability and structural information are the same as in Fig. 1.

Fig. 1. Predicted phase velocity dispersion for dilatational waves of the first kind in snow.

- (A)  $\rho = 210 \text{ kg/m}^3$ ,  $B = 1.5 \times 10^{-4} \text{ s m}^3/\text{kg}$ ,  $\Upsilon = 2.86$ ,  
 (B)  $\rho = 300 \text{ kg/m}^3$ ,  $B = 1.3 \times 10^{-4} \text{ s m}^3/\text{kg}$ ,  $\Upsilon = 2.86$ ,  
 (C)  $\rho = 410 \text{ kg/m}^3$ ,  $B = 0.9 \times 10^{-4} \text{ s m}^3/\text{kg}$ ,  $\Upsilon = 2.86$ ,  
 (D)  $\rho = 508 \text{ kg/m}^3$ ,  $B = 0.3 \times 10^{-4} \text{ s m}^3/\text{kg}$ ,  $\Upsilon = 2.86$ .

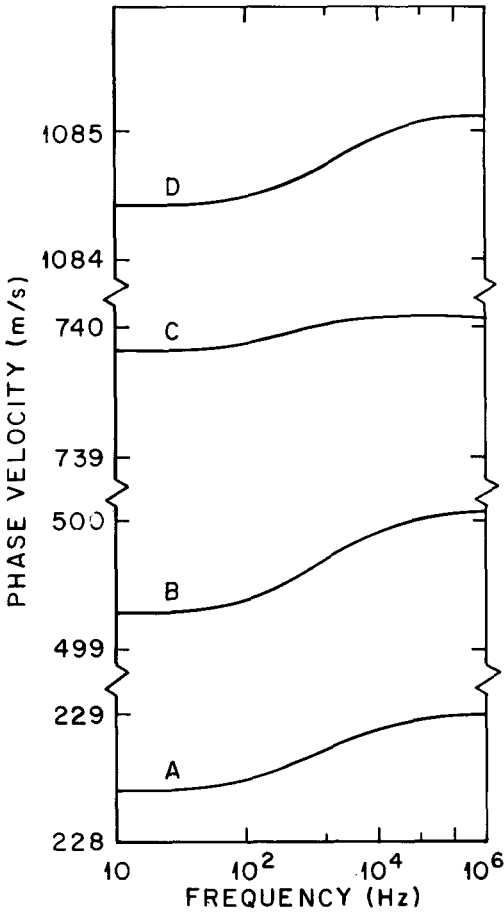


Fig. 3. Predicted phase velocity dispersion for shear waves in snow. The density, permeability and structural information are the same as in Fig. 1.

decrease with increasing snow density (Fig. 2). Amplitude attenuation is controlled by and increases with frequency, density and decreasing air permeability (Figs. 4, 7 and 10).

Calculated wave impedances for snow of different

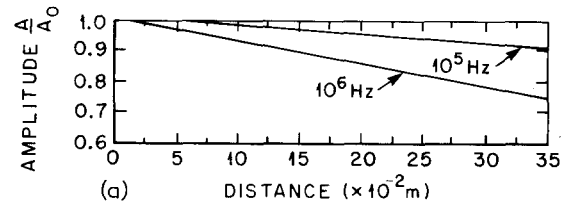
Fig. 4(a). Predicted amplitude attenuation of shear waves in snow.  $\rho = 210 \text{ kg/m}^3$ ,  $B = 1.5 \times 10^{-4} \text{ s m}^3/\text{kg}$ ,  $\tau = 2.86$ .  $A_0$  is the wave amplitude at a distance of 0 m.

Fig. 4(b). Predicted amplitude attenuation of dilatational waves of the first kind (fast waves) and dilatational waves of the second kind (slow waves) in snow.  $\rho = 210 \text{ kg/m}^3$ ,  $B = 1.5 \times 10^{-4} \text{ s m}^3/\text{kg}$ ,  $\tau = 2.86$ .

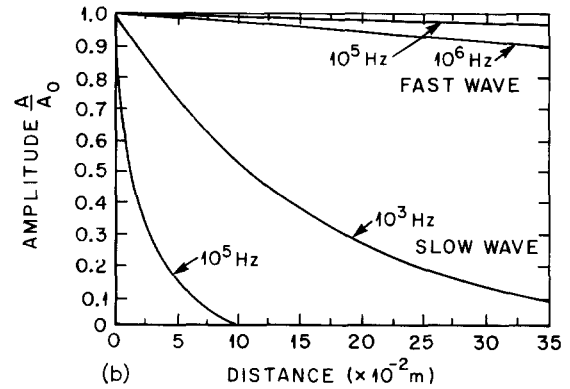
Fig. 4(c). Predicted amplitude attenuation of shear waves in snow.  $\rho = 508 \text{ kg/m}^3$ ,  $B = 0.2 \times 10^{-4} \text{ s m}^3/\text{kg}$ ,  $\tau = 2.86$ .

Fig. 4(d). Predicted amplitude attenuation of dilatational waves of the first kind and dilatational waves of the second kind.  $\rho = 508 \text{ kg/m}^3$ ,  $B = 0.2 \times 10^{-4} \text{ s m}^3/\text{kg}$ ,  $\tau = 2.86$ .

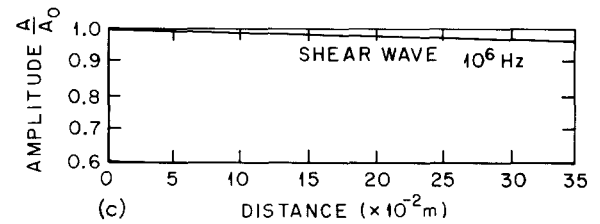
air permeabilities and densities are shown in Fig. 11, in which the ratio between the wave impedance for snow and the characteristic impedance of air is plotted against frequency. These nondimensional curves indicate that the impedance of snow differs little from that of air. This would explain the strong acoustic absorption characteristics of snow (Oura, 1952b; Ishida, 1965; Johnson, 1978), and implies



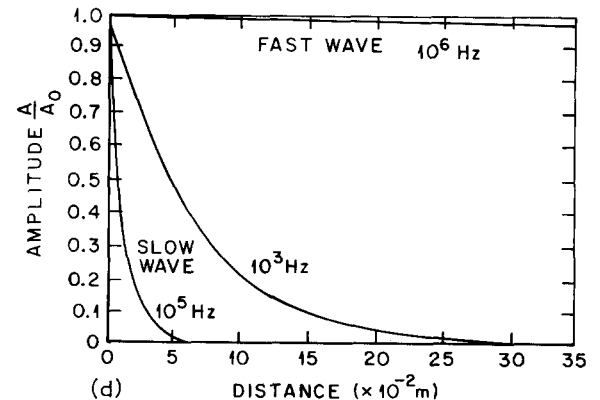
(a)



(b)



(c)



(d)

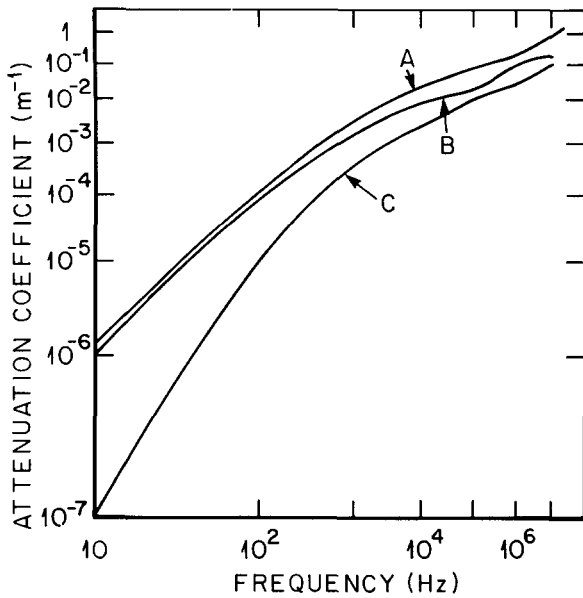


Fig. 5. Predicted attenuation coefficients for dilatational waves of the first kind.

(A)  $\rho = 210 \text{ kg/m}^3$ ,  $B = 1.5 \times 10^{-4} \text{ s m}^3/\text{kg}$ ,  $\gamma = 2.86$ ,  
 (B)  $\rho = 300 \text{ kg/m}^3$ ,  $B = 1.3 \times 10^{-4} \text{ s m}^3/\text{kg}$ ,  $\gamma = 2.86$ ,  
 (C)  $\rho = 508 \text{ kg/m}^3$ ,  $B = 0.3 \times 10^{-4} \text{ s m}^3/\text{kg}$ ,  $\gamma = 2.86$ .

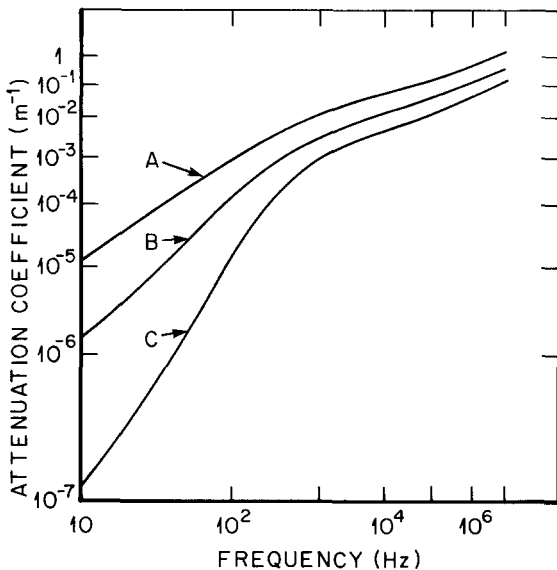


Fig. 6. Predicted attenuation coefficients for shear waves in snow. Density, permeability and structural information are the same as in Fig. 5.

that a large portion of the acoustic energy transmitted across an air/snow interface is transmitted through the pore system as waves of the second kind.

The present theory neglects the effects of internal friction within the ice skeleton which may be significant for low density snow (Gubler, personal com-

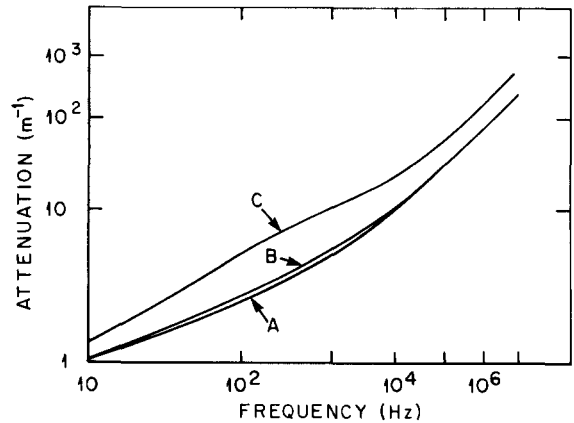


Fig. 7. Predicted attenuation coefficients for dilatational waves of the second kind in snow. Density, permeability and structural information are the same as in Fig. 5.

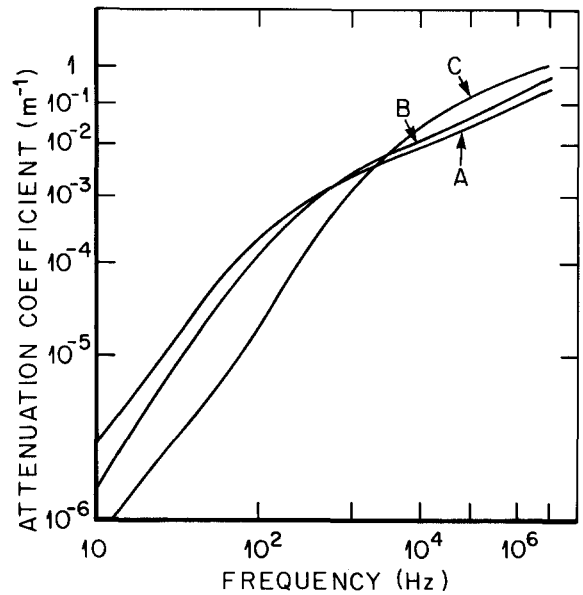


Fig. 8. The predicted influence of air permeability on the attenuation of dilatational waves of the first kind.

(A)  $\rho = 210 \text{ kg/m}^3$ ,  $B = 3.6 \times 10^{-4} \text{ s m}^3/\text{kg}$ ,  $\gamma = 2.31$ ,  
 (B)  $\rho = 210 \text{ kg/m}^3$ ,  $B = 1.5 \times 10^{-4} \text{ s m}^3/\text{kg}$ ,  $\gamma = 2.31$ ,  
 (C)  $\rho = 210 \text{ kg/m}^3$ ,  $B = 0.2 \times 10^{-4} \text{ s m}^3/\text{kg}$ ,  $\gamma = 2.31$ .

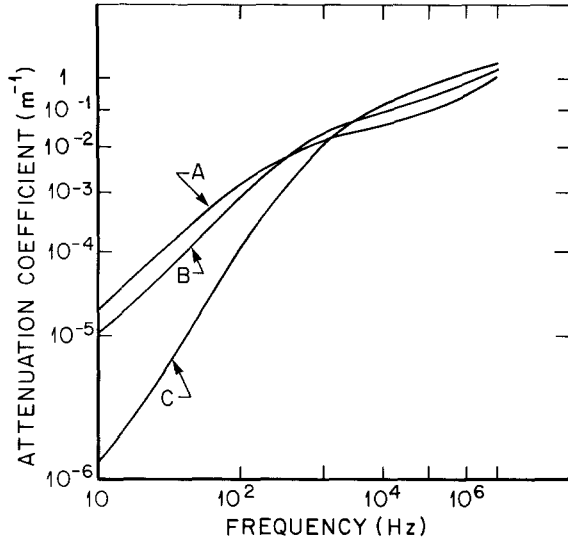


Fig. 9. The predicted influence of air permeability on the attenuation coefficients for shear waves. Density, permeability and structural information are the same as in Fig. 8.

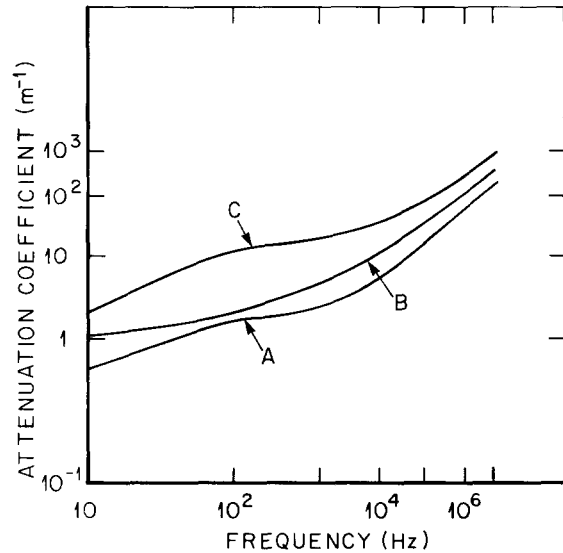


Fig. 10. The predicted influence of air permeability on the attenuation coefficients for dilatational waves of the second kind. Density, permeability and structural information are the same as in Fig. 8.

munication). These effects can be treated by assuming that the ice skeleton is a viscoelastic material in the phenomenological sense. The equations of motion describing a porous material can then be modified by using operators to incorporate internal solid dissipation mechanisms as outlined by Biot (1962a, 1962b).

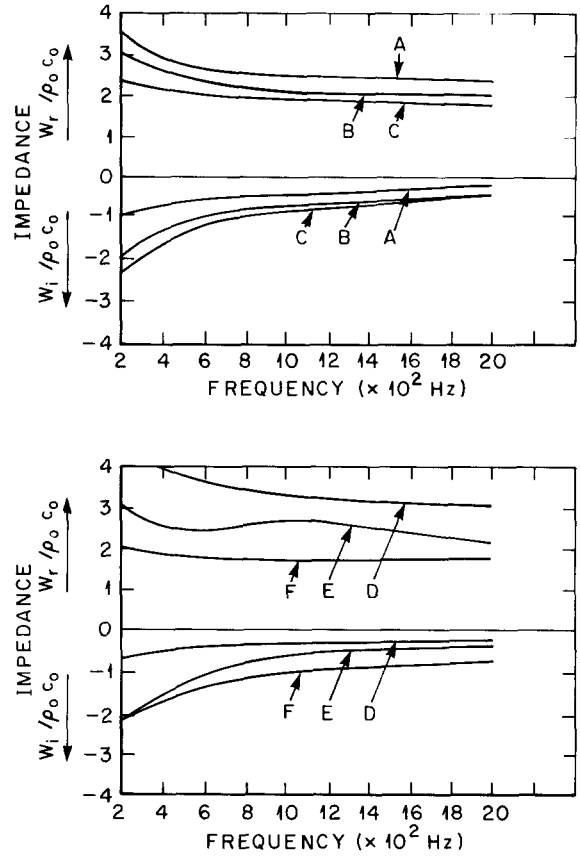


Fig. 11. Predicted wave impedance for snow.  
 (A)  $\rho = 410 \text{ kg/m}^3$ ,  $B = 1.0 \times 10^{-4} \text{ s m}^3/\text{kg}$ ,  $\tau = 2.86$ ,  
 (B)  $\rho = 210 \text{ kg/m}^3$ ,  $B = 3.6 \times 10^{-4} \text{ s m}^3/\text{kg}$ ,  $\tau = 2.86$ ,  
 (C)  $\rho = 210 \text{ kg/m}^3$ ,  $B = 1.0 \times 10^{-4} \text{ s m}^3/\text{kg}$ ,  $\tau = 2.86$ ,  
 (D)  $\rho = 410 \text{ kg/m}^3$ ,  $B = 0.9 \times 10^{-4} \text{ s m}^3/\text{kg}$ ,  $\tau = 2.86$ ,  
 (E)  $\rho = 350 \text{ kg/m}^3$ ,  $B = 1.0 \times 10^{-4} \text{ s m}^3/\text{kg}$ ,  $\tau = 2.86$ ,  
 (F)  $\rho = 210 \text{ kg/m}^3$ ,  $B = 4.9 \times 10^{-4} \text{ s m}^3/\text{kg}$ ,  $\tau = 2.86$ .

**PREDICTED ACOUSTICAL RESPONSE COMPARED TO AVAILABLE TEST DATA**

The experimental results of several authors are used in this section in a general comparison between observed and theoretical acoustic wave phenomena in snow. Unfortunately, little experimental data are available to use in a direct comparison with the theoretical results. No data have been published showing both experimentally determined phase velocity dispersion and attenuation characteristics for snow. Some experimental phase velocity data are available from the work of Oura (1952a), Smith (1965), Yamada et al. (1974), Bogorodskii et al. (1974), and others. These can be used to illustrate

TABLE 2

A comparison between experimentally determined wave propagation velocities (from <sup>1</sup>Öuru, 1952a, <sup>2</sup>Smith, 1965, <sup>3</sup>Yamada et al., 1974, and <sup>4</sup>Bogorodskii et al., 1974) and theoretically calculated phase velocities for snow

Density (kg/m <sup>3</sup> )	Experimental phase velocity (m/s)			Theoretical phase velocity (m/s)		
	Fast wave	Slow wave	Shear wave	Dilatational wave of the first kind	Dilatational wave of the second kind	Shear wave
125	—	277 <sup>1</sup>	—	—	—	—
210	500 <sup>3</sup>	256 <sup>1</sup>	229 <sup>3</sup>	496	282.7	228.9
250	625 <sup>3</sup>	245 <sup>1</sup>	375 <sup>3</sup>	621.6	273.7	373.9
256	—	254 <sup>4</sup>	—	—	—	—
280	—	207 <sup>1</sup>	—	—	—	—
288	—	242 <sup>4</sup>	—	—	—	—
300	1000 <sup>3</sup>	—	500 <sup>3</sup>	1000	273.7	500
305	—	285 <sup>4</sup>	—	—	—	—
400	—	180 <sup>1</sup>	—	—	—	—
410	1270 <sup>2</sup>	—	746 <sup>2</sup>	1270.1	273.1	740.5
440	1312 <sup>2</sup>	—	758 <sup>2</sup>	1312.8	271.4	758.5
508	1637 <sup>2</sup>	—	1085 <sup>2</sup>	1637	269.9	1085.1
551	2225 <sup>2</sup>	—	1265 <sup>2</sup>	2225.3	268.4	1265.1
600	2518 <sup>2</sup>	—	1321 <sup>2</sup>	2520.4	269.4	1323

the general similarity between the experimental results and theory. Table 2 summarizes and compares some of the existing experimental phase velocity data with the theoretically predicted high frequency values. This should be a realistic comparison because the experimental measurements were made using either explosive or high frequency acoustical sources. The various experimental techniques were not designed to distinguish between dilatational waves of the first and second kind. However, the measured phase velocities for dilatational waves can be organized into two distinct velocity categories which are similar to those predicted by theory. The measured shear wave velocities for snow are in good agreement with theoretical predictions. The good agreement between experimental and calculated propagation velocities for dilatational waves of the first kind and shear waves is to be expected. The mechanical parameters for the porous media model were calculated using the experimental propagation velocity results for shear and compression waves which are directly related to the dilatational waves of the first kind and shear waves in Biot's theory. The measured propagation velocities for slow waves agree qualitatively with calculated values for dilatational waves of the second kind. Both the measured and calculated propagation velocities are relatively low and decrease with increasing snow density.

A quantitative comparison is not possible since the parameters describing the snow in Öuru's (1952a) and Bogorodskii et al.'s (1974) experiments were not given.

No data are available for attenuation of dilatational waves of the first and second kind and shear waves in snow. Transmission loss experiments using dilatational waves have been conducted by a number of investigators in an effort to determine the attenuation characteristics of acoustic waves in snow (Ishida, 1965; Lang, 1976; Johnson, 1978). These experiments were not capable of examining the attenuation characteristics for each of the two dilatational waves because the effects of coupling between the air and the ice framework were unknown. Pressure changes, which according to theory are due to the coupled influence of dilatational waves of the first and second kind (eqns. (1) and (4)), were used to determine transmission losses. This means that the existing transmission loss measurements include the coupled influence of the two dilatational wave types. Additionally, in some cases the experimental setups were such that reflections at boundaries and geometrical losses associated with the use of point acoustic sources further complicated the interpretation of measurements (Ishida, 1965; Lang, 1976). Johnson (1978) has conducted transmission loss experiments on snow using a wave tube to generate acoustic plane

waves and a traveling probe microphone to measure the acoustic wave pressure. Such an experiment is still not able to examine the attenuation of each wave type but does eliminate boundary reflection and geometrical attenuation problems. Johnson's measurements are useful in that the plane wave attenuation of the coupled dilatational waves propagating in the air pores can be compared between theory and experiment in a relative fashion. The air pressure within the pore system of snow can be calculated from eqn. (1) and for one dimension is

$$s = Q\partial u_1/\partial x_1 + R\partial U_1/\partial x_1 \tag{8}$$

where  $u$  and  $U$  are defined by eqns. (4) and (5). The coupling influence of dilatational waves of the first and second kind on the air pressure wave is apparent from eqns. (4) and (8). This coupling accounts for the form of the theoretically predicted amplitude decay of the air pressure plane waves (Fig. 12). Preliminary attenuation measurements of air pressure plane waves by Johnson (1978) (Figs. 13(a) and 13(b)) are similar to those of Fig. 12. These results indicate that an air pressure wave is strongly attenuated near the snow/air interface (acoustic energy transmitted from air into snow) and attenuated to a lesser extent away from the interface. The theoretical description implies that dilatational waves of the second kind are responsible for the strong attenuation effects. More experiments are needed to

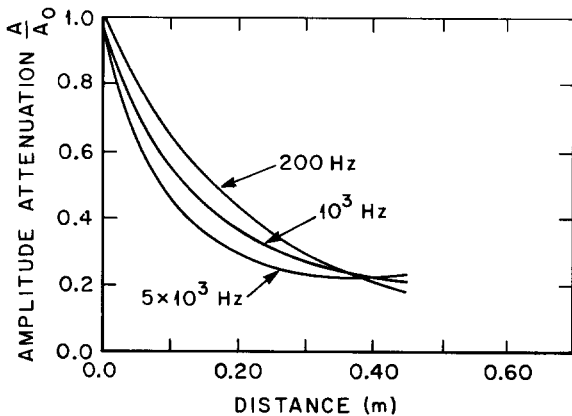


Fig. 12. Predicted amplitude attenuation of planar air pressure waves in snow using Biot's model.  $\rho = 210 \text{ kg/m}^3$ ,  $B = 1.5 \times 10^{-4} \text{ s m}^3/\text{kg}$ ,  $\gamma = 2.86$ . Pressure wave calculations are from  $s = Qe + Re$ .  $A_0$  is the wave amplitude at a distance of 0 m.

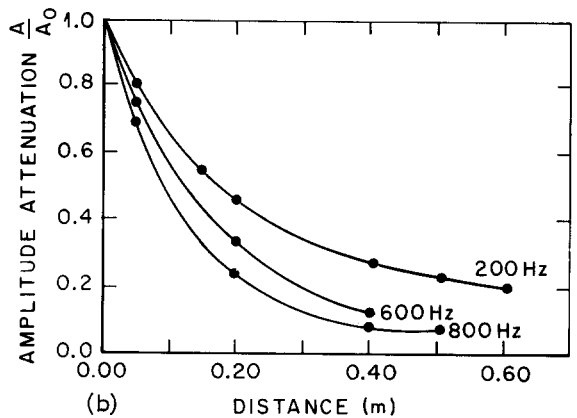
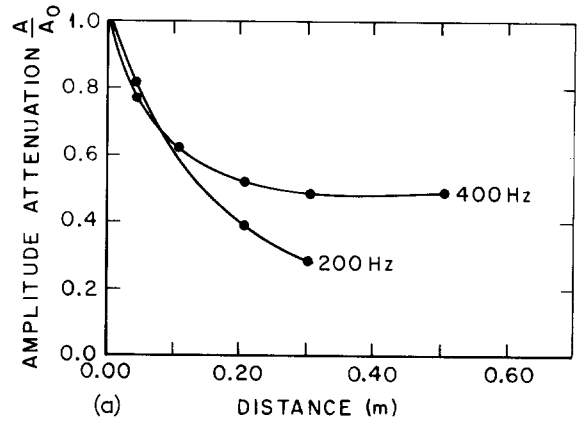


Fig. 13(a). Measured amplitude attenuation of planar air pressure waves in snow.  $\rho = 230 \text{ kg/m}^3$ ,  $B = 1.3 \times 10^{-4} \text{ s m}^3/\text{kg}$ .  $A_0$  is the wave amplitude at a distance of 0 m.

Fig. 13(b). Measured amplitude attenuation of planar air pressure waves in snow.  $\rho = 230 \text{ kg/m}^3$ ,  $B = 1.3 \times 10^{-4} \text{ s m}^3/\text{kg}$ .

determine accurately the attenuation characteristics of acoustic waves in snow.

Wave impedance measurements have been made by Johnson (1978) using a wave tube abutted against homogeneous snow layers. Figure 14 shows experimental wave impedance data for several different snow layers. These measurements are similar to the theoretical curves of Fig. 11 and further illustrate that snow is a low impedance, highly absorbing material. The impedance data for snow support the theoretical predictions that the acoustic properties of snow are strongly affected by the air-filled pore system.

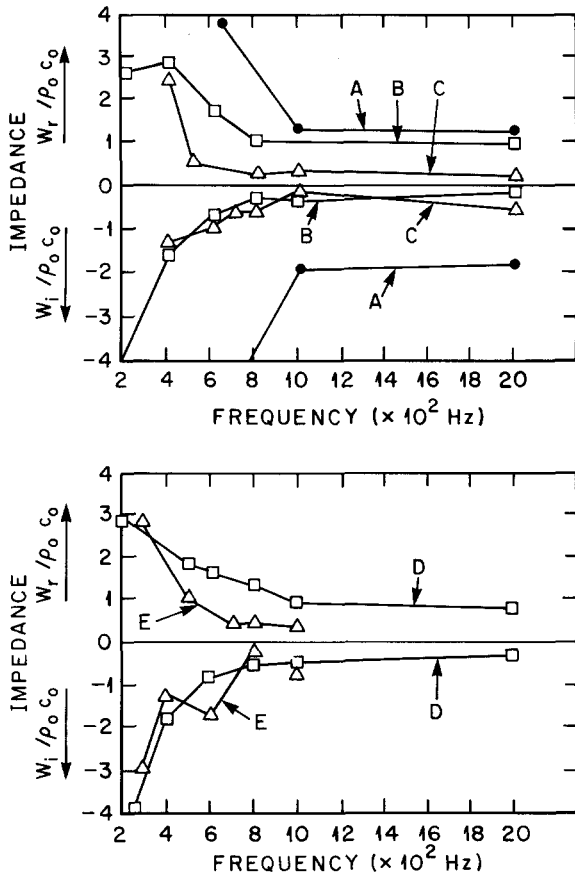


Fig. 14. Measured wave impedance for naturally deposited snow.

- (A)  $\rho = 420 \text{ kg/m}^3$ ,  $B = 1.2 \times 10^{-4} \text{ s m}^3/\text{kg}$ ,  
 (B)  $\rho = 200 \text{ kg/m}^3$ ,  $B = 4.9 \times 10^{-4} \text{ s m}^3/\text{kg}$ ,  
 (C)  $\rho = 200 \text{ kg/m}^3$ ,  $B = 1.5 \times 10^{-4} \text{ s m}^3/\text{kg}$ ,  
 (D)  $\rho = 350 \text{ kg/m}^3$ ,  $B = 0.5 \times 10^{-4} \text{ s m}^3/\text{kg}$ ,  
 (E)  $\rho = 210 \text{ kg/m}^3$ ,  $B = 2.17 \times 10^{-4} \text{ s m}^3/\text{kg}$ .

A lack of experimental data limits the extent to which a theory for acoustic wave propagation in snow can be tested and improved. There is a great need at present for accurate phase velocity dispersion, amplitude attenuation and wave impedance measurements for each of the wave types identified by the model.

## CONCLUSIONS

Biot's (1956a, 1956b) model for acoustic wave propagation in an elastic fluid-filled porous media has been used to describe wave propagation in snow.

This theory predicts the existence of two dilatational waves and a shear wave in snow. The two dilatational waves are uncoupled from one another but involve coupled motion between the air and ice skeleton. Dilatational waves of the first kind and shear waves are only slightly dispersive and attenuated with distance. Dilatational waves of the second kind are strongly dispersive and highly attenuated. The theory also indicates that the wave impedance for snow is relatively close to that of air differing, over a range of values, by less than a factor of five (Fig. 11). This indicates that a large portion of the acoustic wave energy is transmitted into snow through the air pores as dilatational waves of the second kind.

Accurate experimental measurements of phase velocity, amplitude attenuation and wave impedance are required to test the theory. Such experimental data are not presently available. The experimental data which do exist tend to support the general predictions of the theory. Phase velocity measurements for snow are in the same range as those predicted by theory for the two dilatational waves and shear waves, as are attenuation measurements of air pressure plane waves in snow and wave impedance measurements.

## ACKNOWLEDGEMENTS

The author wishes to thank Dr. L. Shapiro, D.K. Perovich, and Dr. T. Lang and an anonymous reviewer for their helpful comments and suggestions.

This work was completed at the University of Washington, Geophysics program, with the support of the Washington State Highway Department under Contract No. Y-1637.

## REFERENCES

- Biot, M.A. (1941), General theory of three dimensional consolidation, *J. Appl. Phys.*, 12: 155-164.  
 Biot, M.A. (1956a), Theory of propagation of elastic waves in a fluid-saturated porous solid. I. Low frequency range, *J. Acoust. Soc. Am.*, 28(2): 168-178.  
 Biot, M.A. (1956b), Theory of propagation of elastic waves in a fluid-saturated porous solid. II. Higher frequency range, *J. Acoust. Soc. Am.*, 28(2): 179-191.  
 Biot, M.A. (1962a), Mechanics of deformation and acoustic propagation in porous media, *J. Appl. Phys.*, 33(4): 1482-1498.

- Biot, M.A. (1962b), Generalized theory of acoustic propagation in porous dissipative media, *J. Acoust. Soc. Am.*, 34(9): 1254–1264.
- Biot, M.A. and Willis, D.B. (1957), The elastic coefficients of the theory of consolidation, *J. Appl. Phys.*, 24, Trans. ASME, Series E, 79: 594–601.
- Bogorodskii, V.V., Gavrilov, V.P. and Nikitin, V.A. (1974), Characteristics of sound propagation in snow, *Akust. Zh.*, 20: 195–198 (*Sov. Phys. Acoust.*, 20(2): 121–122).
- Chae, Y.S. (1966), Frequency dependence of dynamic moduli of, and damping in, snow. In: *Physics of Snow and Ice*, H. Ōura (Ed.), Int. Conf. on Low Temperature Science, Proc. Vol. I, Part 2: 827–842, Institute of Low Temperature Science, Hokkaido University, Sapporo, Japan, 1967.
- Deresiewicz, H. and Rice, J.T. (1962), The effect of boundaries on wave propagation in a liquid filled porous solid. III. Reflection of plane waves at a free plane boundary (general case), *Bull. Seismol. Soc. Am.*, 52(3): 595–625.
- Gubler, H. (1977), Artificial release of avalanches by explosives, *J. Glaciol.*, 19(81): 419–429.
- Ishida, T. (1965), Acoustic properties of snow, *Contributions from the Institute of Low Temperature Science, Series A*, 20: 23–68.
- Johnson, J.B. (1978), unpublished, Stress waves in snow, Ph.D. Thesis, University of Washington, 148 pp.
- Johnson, J.B. (1980), A model for snow-slab failure under conditions of dynamic loading, *J. Glaciol.*, 26(94): 245–254.
- Lang, T.E. (1976), Measurements of acoustical properties of hard-pack snow, *J. Glaciol.*, 17(76): 269–276.
- Mellor, M. (1964), Properties of snow, U.S. Cold Regions Research and Engineering Lab., Hanover, N.H., III. A1, Part III Engineering, Section A: Snow Engineering, 105 p.
- Mellor, M. (1974), A Review of basic snow mechanics, Proc. of the Grindelwald Symp., April 1974, IAHS–AISH Publication No. 114, pp. 251–291.
- Nakaya, U. (1959a), Visco-elastic properties of snow and ice in the Greenland ice cap, U.S. Snow, Ice and Permafrost Research Establishment, Research Report 46, 33 pp.
- Nakaya, U. (1959b), Visco-elastic properties of processed snow, U.S. Snow, Ice and Permafrost Establishment, Research Report 58, 22 pp.
- Nakaya, U. (1961), Elastic properties of processed snow with reference to its internal structure, U.S. Cold Regions Research and Engineering Lab., Hanover, N.H., Research Report 82, 25 pp.
- Ōura, H. (1952a), Sound velocity in the snow cover, *Low Temp. Sci.*, 9: 171–178.
- Ōura, H. (1952b), Reflection of sound at snow surface and mechanism of sound propagation in snow, *Low Temp. Sci.*, 9: 179–186.
- Smith, J.L. (1965), The elastic constants, strength and density of Greenland snow as determined from measurements of sonic wave velocity, U.S. Cold Regions Research and Engineering Lab., Hanover, N.H., Tech. Rept. 167, 18 pp.
- Smith, N. (1969), Determining the dynamic properties of snow and ice by forced vibration, U.S. Cold Regions Research and Engineering Lab., Hanover, N.H., Tech. Rept. 216, 17 pp.
- Yamada, T., Hasemi, T., Izumi, K. and Sata, A. (1974), On the dependencies of the velocities of *P* and *S* waves and thermal conductivity of snow upon the texture of snow, *Contributions from the Institute of Low Temperature Science, Ser. A*, 32: 71–80.
- Yen, Y.C. and Fan, S.S.T. (1966), Pressure wave propagation in snow with non-uniform permeability, U.S. Cold Regions Research and Engineering Lab., Hanover, N.H., Research Report 210, 9 pp.
- Yew, C.H. and Jogi, P.N. (1976), Study of wave motion in fluid saturated porous rocks, *J. Acoust. Soc. Am.*, 60(1): 2–8.
- Yew, C.H. and Jogi, P.N. (1978), The determination of Biot's parameters for sandstones. Part I: Static tests, *Exp. Mech.*, 18(5): 167–172.